Review of "Projections of oceanic N_2O emissions in the 21st century using the IPSL Earth System Model" by Martinez-Rey et al.

The Authors addressed most of my comments in the revised version of the manuscript, and I'm generally satisfied with the changes and additions. In particular, the discussion of the potential shortcomings of the IPSL model, and the implications for the analysis, have been substantially expanded in the revised manuscript. The description of the N_2O production parameterizations, their origin and rationale have been also clarified, and references have been provided.

Among the conclusions of the paper, the suggested increase in subsurface inventories because of increased stratification (and despite reduced production) is novel and thought provoking. The decrease in interior N_2O production as a response to decreased export and remineralization is also interesting, but more in line with our expectations. The role and importance of oxygen minimum zones and suboxic waters, and of the low-O_2 production pathway, is still unclear, and perhaps leads to the least robust results of the paper. However, this reflects the uncertainty that still exists in our understanding of low-O_2 processes, and the shortcomings of the 3D GCM utilized. These limitations have been now thoroughly acknowledged by the Authors.

I think that the manuscript will be a useful first reference for anyone interested in the future evolution of N_2O emission under climate change. It also points to processes that should be robust and of first order importance in Earth System Models (and presumably in the real world), and it suggests several aspects of the N_2O cycle where more work is needed.

We thank the referee for the second review of the manuscript. We acknowledge indeed the improvements in the manuscript on the above mentioned topics thanks to the comments from the referees.

I still have few concerns regarding the box model formulation. I realize this is not an essential part of the paper, although it is used to gain some insight to interpret the GCM model behavior. Also, my concerns might not change the final message. However, equations 2-3, with the parameters explained in the revised text and Table S1, seem wrong as a box model of the surface and deep ocean. My problems are:

To be dimensionally consistent, and obtain rates of change (as in the left hand sides), both the mixing coefficient and the gas exchange parameter should have units of (1/time). For example, a simple interpretation would hold if the mixing coefficient was a volume transport (m3/s) divided by the box volume (m3), and the gas exchange coefficient a piston velocity (m/s) multiplied by the box surface area (m2) and divided by the box volume (m3). As they are now, expressed as dimensional fractions, these coefficients do not allow to calculate time rates of changes, and the box model does not have a clear physical meaning. Once one realizes that the mixing terms represent a volume transport divided by the volume of the box, the mixing coefficients (v) should not be the same for the surface and deep box - a given transport of water will have much smaller effects in the deep box because of the much larger volume - unless here the surface and deep volumes are equal, which I guess the Authors could have (somewhat oddly) assumed (in which case the surface gas exchange should be quite small, because of the thickness of the surface box).

Similarly the gas exchange term is puzzling - even after correcting for the units of k (or pi) (which dimensionally should not be a fraction), the atmospheric concentrations are missing - it looks like the surface box just outgasses N_2O to an atmosphere with zero mixing ratio (not a big effect but physically odd).

I suggest that the authors check their model formulation, or at least provide a consistent physical interpretation and derivation of the equations.

The comment from the referee made us aware of how misleading is the box model as it stands. The main purpose of the box model was to synthesize the GCM model behaviour and basically to simplify the description of the main mechanisms leading to changes in future N_2O emissions. However, it is clear that it is not the case and therefore we have decided to withdraw the box model analysis from the manuscript. We think that the main messages of the paper are still well explained and comprehensible without the box model.

Technical:

l. 353: initialize (typo)

l. 385: decrease increase: awkward wording

l. 487: smaller instead of less

These proposed changes have been included in the latest version of the manuscript, which is attached below with corrections marked in blue.

"Projections of oceanic N_2O emissions in the 21st century using the IPSL Earth System Model"

J. Martinez-Rey[1], L. Bopp[2], M. Gehlen[3], A. Tagliabue[4] and N. Gruber[5].

[1] Laboratoire des Sciences du Climat et de l'Environnement, IPSL, CEA/CNRS/UVSQ, Bat. 712 - Orme des Merisiers, F-91191 CE Saclay, Gif-sur-Yvette, France.
jorge.martinez-rey@lsce.ipsl.fr

[2] Laboratoire des Sciences du Climat et de l'Environnement, IPSL, CEA/CNRS/UVSQ, Bat. 712 - Orme des Merisiers, F-91191 CE Saclay, Gif-sur-Yvette, France.
laurent.bopp@lsce.ipsl.fr

[3] Laboratoire des Sciences du Climat et de l'Environnement, IPSL, CEA/CNRS/UVSQ, Bat. 712 - Orme des Merisiers, F-91191 CE Saclay, Gif-sur-Yvette, France.
marion.gehlen@lsce.ipsl.fr

[4] School of Environmental Sciences, University of Liverpool, 4 Brownlow Street, Liverpool L69 3GP, UK.
a.tagliabue@liverpool.ac.uk

[5] Environmental Physics, Institute of Biogeochemistry and Pollutant Dynamics, ETH, CHN E31.2, Universitaetstrasse 16, 8092 Zürich, Switzerland.
nicolas.gruber@env.ethz.ch

0. Abstract

The ocean is a substantial source of nitrous oxide (N_2O) to the atmosphere, but little is known on how this flux might change in the future. Here, we investigate the potential evolution of marine N_2O emissions in the 21st century in response to anthropogenic climate change using the global ocean biogeochemical model NEMO-PISCES. Assuming nitrification as the dominant N_2O formation pathway, we implemented two different parameterizations of N_2O production which differ primarily at low oxygen (O_2) conditions. When forced with output from a climate model simulation run under the business-as-usual high CO_2 concentration scenario (RCP8.5), our simulations suggest a decrease of 4 to 12 % in N_2O emissions from 2005 to 2100, i.e., a reduction from 4.03 / 3.71 to 3.54 / 3.56 TgN yr^{-1} depending on the parameterization. The emissions decrease strongly in the western basins of the Pacific and Atlantic oceans, while they tend to increase above the Oxygen Minimum Zones (OMZs), i.e., in the Eastern Tropical Pacific and in the northern Indian Ocean. The reduction in N_2O emissions is caused on the one hand by weakened nitrification as a consequence of reduced primary and export production, and on the other hand by stronger vertical stratification, which reduces the transport of N_2O from the ocean interior to the ocean surface. The higher emissions over the OMZ are linked to an expansion of these zones under global warming, which leads to increased N_2O production associated primarily with denitrification. While there are many uncertainties in the relative contribution and changes in the N_2O production pathways, the increasing storage seems unequivocal and determines largely the decrease in N_2O emissions in the future. From the perspective of a global climate system, the averaged feedback strength associated with the projected decrease in oceanic N_2O emissions amounts to around -0.009 W m^{-2}K^{-1}, which is comparable to the potential increase from terrestrial N_2O sources. However, the assesment for a compensation between the terrestrial and marine feedbacks calls for an improved representation of N_2O production terms in fully coupled next generation of Earth System Models.

1 Introduction

Nitrous oxide (N_2O) is a gaseous compound responsible for two key feedback mechanisms within the Earth's climate. First, it acts as a long-lived and powerful greenhouse gas (Prather et al., 2012) ranking third in anthropogenic radiative forcing after carbon dioxide (CO_2) and methane (CH_4) (Myrhe et al., 2013). Secondly, the ozone (O_3) layer depletion in the future might be driven mostly by N_2O after the drastic reductions in CFCs emissions start to show their effect on stratospheric chlorine levels (Ravishankara et al., 2009). The atmospheric concentration of N_2O is determined by the natural balance between sources from land and ocean and the destruction of N_2O in the atmosphere largely by photolysis (Crutzen, 1970; Johnston, 1971). The natural sources from land and ocean amount to ~6.6 and 3.8 TgN yr^{-1}, respectively (Ciais et al., 2013). Anthropogenic activities currently add an additional 6.7 TgN yr^{-1} to the atmosphere, which has caused atmospheric N_2O to increase by 18% since pre-industrial times (Ciais et al., 2013), reaching 325 ppb in the year 2012 (NOAA ESRL Global Monitoring Division, Boulder, Colorado, USA, http://esrl.noaa.gov/gmd/).

Using a compilation of 60,000 surface ocean observations of the partial pressure of N_2O (pN_2O), Nevison et al. (2004) computed a global ocean source of 4 TgN yr^{-1}, with a large range of uncertainty from 1.2 to 6.8 TgN yr^{-1}. Model derived estimates also differ widely, i.e., between 1.7 and 8 TgN yr^{-1} (Nevison et al., 2003; Suntharalingam et al., 2000). These large uncertainties are a consequence of too few observations and of poorly known N_2O formation mechanisms, reflecting a general lack of understanding of key elements of the oceanic nitrogen cycle (Gruber and Galloway, 2008; Zehr and Ward, 2002), and of N_2O in particular (e.g., Zamora et al., 2012, Bange et al., 2009 or Freing et al., 2012, among others). A limited number of interior ocean N_2O observations were made available only recently (Bange et al., 2009), but they contain large temporal and spatial gaps. Information on the rates of many important processes remains insufficient, particularly in natural settings. There are only few studies from a limited number of specific regions such as the Arabian Sea, Central and North Pacific, Black Sea, the Bedford Basin and the Scheldt estuary, which can be used to derive and test model parameterisations (Mantoura et al., 1993; Bange et al., 2000; Elkins et al., 1978; Farias et al., 2007; Frame and Casciotti, 2010; Westley et al., 2006; Yoshida et al., 1989; Punshon

86 and Moore, 2004; De Wilde and De Bie, 2000).
87 N_2O is formed in the ocean interior through two major pathways and consumed only in
88 oxygen minimum zones through denitrification (Zamora et al., 2012). The first
89 production pathway is associated with nitrification (conversion of ammonia, NH_4^+, into
90 nitrate, NO_3^-), and occurs when dissolved O_2 concentrations are above 20 µmol L^{-1}. We
91 subsequently refer to this pathway as the high-O_2 pathway. The second production
92 pathway is associated with a series of processes when O_2 concentrations fall below ~5
93 µmol L^{-1} and involve a combination of nitrification and denitrification (hereinafter
94 referred to as low-O_2 pathway) (Cohen and Gordon, 1978; Goreau et al., 1980; Elkins et
95 al., 1978). As nitrification is one of the processes involved in the aerobic remineralization
96 of organic matter, it occurs nearly everywhere in the global ocean with a global rate at
97 least one order of magnitude larger than the global rate of water column denitrification
98 (Gruber, 2008). A main reason is that denitrification in the water column is limited to
99 the OMZs, which occupy only a few percent of the total ocean volume (Bianchi et al.,
100 2012). This is also the only place in the water column where N_2O is being consumed.
101 The two production pathways have very different N_2O yields, i.e., fractions of nitrogen-
102 bearing products that are transformed to N_2O. For the high-O_2 pathway, the yield is
103 typically rather low, i.e., only about 1 in several hundred molecules of ammonium
104 escapes as N_2O (Cohen and Gordon, 1979). In contrast, in the low-O_2 pathway, and
105 particularly during denitrification, this fraction may go up to as high as 1:1, i.e., that all
106 nitrate is turned into N_2O (Tiedje, 1988). The relative contribution of the two pathways
107 to global N_2O production is not well established. Sarmiento and Gruber (2006)
108 suggested that the two may be of equal importance, but more recent estimates suggest
109 that the high-O_2 production pathway dominates global oceanic N_2O production (Freing
110 et al., 2012).
111 Two strategies have been pursued in the development of parameterizations for N_2O
112 production in global biogeochemical models. The first approach builds on the
113 importance of the nitrification pathway and its close association with the aerobic
114 remineralization of organic matter. As a result the production of N_2O and the
115 consumption of O_2 are closely tied to each other, leading to a strong correlation between
116 the concentration of N_2O and the apparent oxygen utilization (AOU). This has led to the
117 development of two sets of parameterizations, one based on concentrations, i.e., directly

as a function of AOU (Butler et al., 1989) and the other based on the rate of oxygen utilization, i.e. OUR (Freing et al., 2009). Additional variables have been introduced to allow for differences in the yield, i.e., the ratio of N_2O produced over oxygen consumed, such as temperature (Butler et al., 1989) or depth (Freing et al., 2009). In the second approach, the formation of N_2O is modeled more mechanistically, and tied to both nitrification and denitrification by an O_2 dependent yield (Suntharalingam and Sarmiento, 2000; Nevison et al., 2003; Jin and Gruber, 2003). Since most models do not include nitrification explicitly, the formation rate is actually coupled directly to the remineralization of organic matter. Regardless of the employed strategy, all parameterizations depend to first order on the amount of organic matter that is being remineralized in the ocean interior, which is governed by the export of organic carbon to depth. The dependence of N_2O production on oxygen levels and on other parameters such as temperature only acts at second order. This has important implications not only for the modeling of the present-day distribution of N_2O in the ocean, but also for the sensitivity of marine N_2O to future climate change.

Over this century, climate change will perturb marine N_2O formation in multiple ways. Changes in productivity will drive changes in the export of organic matter to the ocean interior (Steinacher et al., 2010; Bopp et al., 2013) and hence affect the level of marine nitrification. Ocean warming might change the rate of N_2O production during nitrification (Freing et al., 2012). Changes in carbonate chemistry (Bindoff et al., 2007) might cause changes in the C:N ratio of the exported organic matter (Riebesell et al., 2007), altering not only the rates of nitrification, but also the ocean interior oxygen levels (Gehlen et al., 2011). Finally, the expected general loss of oxygen (Keeling et al., 2010; Cocco et al., 2012; Bopp et al., 2013) could substantially affect N_2O production via both nitrifier denitrification and classic denitrification.

Ocean biogeochemical models used for IPCC's 4th assessment report estimated a decrease between 2% and 13% in primary production (PP) under the business-as-usual high CO_2 concentration scenario A2 (Steinacher et al., 2010). A more recent multi-model analysis based on the models used in IPCC's 5th assessment report also suggest a large reduction of PP down to 18% by 2100 for the RCP8.5 scenario (Bopp et al., 2013). In these simulations, the export of organic matter is projected to decrease between 6% and 18% in 2100 (Bopp et al., 2013), with a spatially distinct pattern: in general, productivity and

export are projected to decrease at mid- to low-latitudes in all basins, while productivity and export are projected to increase in the high-latitudes and in the South Pacific subtropical gyre (Bopp et al., 2013). A wider spectrum of responses was reported regarding changes in the ocean oxygen content. While all models simulate decreased oxygen concentrations in response to anthropogenic climate change (by about 2 to 4% in 2100), and particularly in the mid-latitude thermocline regions, no agreement exists with regard to the hypoxic regions, i.e., those having oxygen levels below 60 μmol L^{-1} (Cocco et al., 2012; Bopp et al., 2013). Some models project these regions to expand, while others project a contraction. Even more divergence in the results exists for the suboxic regions, i.e., those having O_2 concentrations below 5 μmol L^{-1} (Keeling et al., 2010; Deutsch et al., 2011; Cocco et al., 2012; Bopp et al., 2013), although the trend for most models is pointing towards an expansion. At the same time, practically none of the models is able to correctly simulate the current distribution of oxygen in the OMZ (Bopp et al., 2013). In summary, while it is clear that major changes in ocean biogeochemistry are looming ahead (Gruber, 2011), with substantial impacts on the production and emission of N_2O, our ability to project these changes with confidence is limited.

In this study, we explore the implications of these future changes in ocean physics and biogeochemistry on the marine N_2O cycle, and make projections of the oceanic N_2O emissions from year 2005 to 2100 under the high CO_2 concentration scenario RCP8.5. We analyze how changes in biogeochemical and physical processes such as net primary production (NPP), export production and vertical stratification in this century translate into changes in oceanic N_2O emissions to the atmosphere. To this end, we use the NEMO-PISCES ocean biogeochemical model, which we have augmented with two different N_2O parameterizations, permitting us to evaluate changes in the marine N_2O cycle at the process level, especially with regard to production pathways in high and low oxygen regimes. We demonstrate that while future changes in the marine N_2O cycle will be substantial, the net emissions of N_2O appear to change relatively little, i.e., they are projected to decrease by about 10% in 2100.

2. Methodology

2.1 NEMO-PISCES Model

Future projections of the changes in the oceanic N_2O cycle were performed using the PISCES ocean biogeochemical model (Aumont and Bopp, 2006) in offline mode with physical forcings derived from the IPSL-CM5A-LR coupled model (Dufresne et al., 2013). The horizontal resolution of NEMO ocean general circulation model is 2° x 2° cos Ø (Ø being the latitude) with enhanced latitudinal resolution at the equator of 0.5°. PISCES is a biogeochemical model with five nutrients (NO_3, NH_4, PO_4, Si and Fe), two phytoplankton groups (diatoms and nanophytoplankton), two zooplankton groups (micro and mesozooplankton), and two non-living compartments (particulate and dissolved organic matter). Phytoplankton growth is limited by nutrient availability and light. Constant Redfield C:N:P ratios of 122:16:1 are assumed (Takahashi et al., 1985), while all other ratios, i.e., those associated with chlorophyll, iron, and silicon (Chl:C, Fe:C and Si:C) vary dynamically.

2.2 N_2O parameterizations in PISCES

We implemented two different parameterizations of N_2O production in NEMO-PISCES. The first one, adapted from Butler et al. (1989) follows the oxygen consumption approach, with a temperature dependent modification of the N_2O yield (P.TEMP). The second one is based on Jin and Gruber (2003) (P.OMZ), following the more mechanistic approach, i.e., it considers the different processes occurring at differing oxygen concentrations in a more explicit manner.

The P.TEMP parameterization assumes that the N_2O production is tied to nitrification only with a yield that is at first order constant. This is implemented in the model by tying the N_2O formation in a linear manner to O_2 consumption. A small temperature dependence is added to the yield to reflect the potential impact of temperature on metabolic rates. The production term of N_2O, i.e., $J^{P.TEMP}(N_2O)$, is then mathematically formulated as:

$$J^{P.TEMP}(N_2O) = (\gamma + \theta\, T\,)\, J(O_2)_{consumption} \quad (1)$$

where γ is a background yield (0.53 x 10^{-4} mol N_2O/mol O_2 consumed), θ is the temperature dependency of γ (4.6 x 10^{-6} mol N_2O (mol O_2)$^{-1}$ K^{-1}), T is temperature (K),

and $J(O_2)_{consumption}$ is the sum of all biological O_2 consumption terms within the model. The same ratio between constants γ and θ is used in the model as in the original formulation from Butler et al. (1989). Although this parameterization is very simple, a recent analysis of N_2O observations supports such an essentially constant yield, even in the OMZ of the Eastern Tropical Pacific (Zamora et al., 2012).

The P.OMZ parameterization, formulated after Jin and Gruber (2003), assumes that the overall yield consists of a constant background yield and an oxygen dependent yield. The former is presumed to represent the N_2O production by nitrification, while the latter is presumed to reflect the enhanced production of N_2O at low oxygen concentrations, in part driven by denitrification, but possibly including nitrification as well. This parameterization includes the consumption of N_2O in suboxic conditions. This gives:

$$J^{P.OMZ}(N_2O) = (\alpha + \beta f(O_2))J(O_2)_{consumption} - k\,N_2O \quad (2)$$

where α is, as in Eq.(1), a background yield ($0.9 \cdot 10^{-4}$ mol N_2O/mol O_2 consumed), β is a yield parameter that scales the oxygen dependent function ($6.2 \cdot 10^{-4}$), $f(O_2)$ is a unitless oxygen-dependent step-like modulating function, as suggested by laboratory experiments (Goreau et al., 1980) (Fig. S1, Supplementary Material), and k is the 1st order rate constant of N_2O consumption close to anoxia (zero otherwise). For k, we have adopted a value of 0.138 yr^{-1} following Bianchi et al. (2012) while we set the consumption regime for O_2 concentrations below 5 µmol L^{-1}. The constant α is in the same order of magnitude as the one proposed by Jin and Gruber (2003), while β is two orders of magnitude smaller. The use of the original value would result in a significant increase of N_2O production associated with OMZs and, hence, in a departure from the assumption of dominant nitrification.

The P.OMZ parameterization permits us the independent quantification of the N_2O formation pathways associated with nitrification and those associated with low-oxygen concentrations (nitrification/denitrification) and their evolution in time over the next century. Specifically, we consider the source term $\alpha\, J(O_2)_{consumption}$ as that associated with the nitrification pathway, while we associated the source term $\beta f(O_2)\, J(O_2)_{consumption}$ with the low-oxygen processes (Fig. S2, Supplementary Material).

N_2O production is inhibited by light in the model, and therefore N_2O production in P.TEMP and P.OMZ parameterizations only occurs below a fixed depth of 100m.

We employ a standard bulk approach for simulating the loss of N_2O to the atmosphere via gas exchange. We use the formulation of Wanninkhof et al. (1992) for estimating the gas transfer velocity, adjusting the Schmidt number for N_2O and using the solubility constants of N_2O given by Weiss and Price (1980). We assume a constant atmospheric N_2O concentration of 284 ppb in all simulations to explore future changes inherent to ocean processes without feedbacks due to changes in the atmosphere.

2.3 Experimental design

NEMO-PISCES was first spun up during 3000 years using constant pre-industrial dynamical forcings fields from IPSL-CM5A-LR (Dufresne et al., 2013) without activating the N_2O parameterizations. This spin-up phase was followed by a 150-yr long simulation, forced by the same dynamical fields now with N_2O production and N_2O sea-to-air flux embedded. The N_2O concentration at all grid points was prescribed initially to 20 nmol L^{-1}, which is consistent with the MEMENTO database average value of 18 nmol L^{-1} below 1500m (Bange et al., 2009). During the 150-yr spin-up, we diagnosed the total N_2O production and N_2O sea-to-air flux and adjusted the α, β, γ and θ parameters in order to achieve a total N_2O sea-to-air flux in the two parameterizations at equilibrium close to 3.85 TgN yr^{-1} (Ciais et al., 2013). In addition, the relative contribution of the high-O_2 pathway in the P.OMZ parameterization was set to 75% of the total N_2O production based on Suntharalingam et al. (2000), where a sensitivity model analysis on the relative contribution of high- and low-O_2 production pathways showed that a higher contribution of nitrification (75%) than denitrification (25%) achieved the best model performance compared to the data product from Nevison et al. (1995). P.TEMP can be considered as 100% nitrification, testing in this way the hypothesis of nitrification as the dominant pathway of N_2O production on a global scale. Nitrification could contribute with up to 93% of the total production based on estimations considering N_2O production along with water mass transport (Freing et al., 2012).

Projections in NEMO-PISCES of historical (from 1851 to 2005) and future (from 2005 to 2100) simulated periods were done using dynamical forcing fields from IPSL-CM5A-LR. These dynamical forcings were applied in an offline mode, i.e. monthly means of

276 temperature, velocity, wind speed or radiative flux were used to force NEMO-PISCES.
277 Future simulations used the business-as-usual high CO_2 concentration scenario (RCP8.5)
278 until year 2100. Century scale model drifts for all the biogeochemical variables presented,
279 including N_2O sea-to-air flux, production and inventory, were removed using an
280 additional control simulation with IPSL-CM5A-LR pre-industrial dynamical forcing
281 fields from year 1851 to 2100. Despite the fact that primary production and the export
282 of organic matter to depth were stable in the control simulation, the air-sea N_2O
283 emissions drifted (an increase of 5 to 12% in 200 yr depending on the parameterization)
284 due to the short spin-up phase (150 yrs) and to the choice of the initial conditions for
285 N_2O concentrations.
286
287 3. Present-day oceanic N_2O
288
289 3.1 Contemporary N_2O fluxes
290
291 The model simulated air-sea N_2O emissions show large spatial contrasts, with flux
292 densities varying by one order of magnitude, but with relatively small differences between
293 the two parameterizations (Fig. 1a and 1b). This is largely caused by our assumption that
294 the dominant contribution (75%) to the total N_2O production in the P.OMZ
295 parameterization is the nitrification pathway, which is then not so different from the
296 P.TEMP parameterization, where it is 100%. As a result, the major part of N_2O is
297 produced in the subsurface via nitrification, contributing directly to imprint changes into
298 the sea-to-air N_2O flux without a significant meridional transport (Suntharalingam and
299 Sarmiento, 2000).
300 Elevated N_2O emission regions (> 50 mgN m^{-2} yr^{-1}) are found in the Equatorial and
301 Eastern Tropical Pacific, in the northern Indian ocean, in the northwestern Pacific, in the
302 North Atlantic and in the Agulhas Current. In contrast, low fluxes (< 10 mgN m^{-2} yr^{-1})
303 are simulated in the Southern Ocean, Atlantic and Pacific subtropical gyres and southern
304 Indian Ocean. The large scale distribution of N_2O fluxes is coherent with Nevison et al.
305 (2004) (Fig. 1c). This comes as a natural consequence of the relatively high contribution
306 of nitrification and hence hotspots of N_2O emissions are associated with regions where
307 higher export of organic matter occurs in the model.

There are however several discrepancies between the model and the data product. At high latitudes, the high N_2O emissions observed in the North Pacific are not well represented in our model, with a significant shift towards the western part of the Pacific basin, similar to other modeling studies (e.g., Goldstein et al., 2003; Jin and Gruber, 2003). The OMZ in the North Pacific, located at approximately 600m deep, is underestimated in the model due to the deficient representation of the Meridional Overturning Circulation (MOC) in the North Pacific in global ocean biogeochemical models, which in turn might suppress low oxygenated areas and therefore one potential N_2O source. Discrepancies between model and observations also occur in the Southern Ocean, a region whose role in global N_2O fluxes remains debated due to the lack of observations and the occurrence of potential artifacts due to interpolation techniques reflected in data products such as that from Nevison et al., 2004. (e.g., Suntharalingam and Sarmiento, 2000, and Nevison et al, 2003). The model also overestimates N_2O emissions in the North Atlantic. The emphasis put on the nitrification pathway suggests that hotspots of carbon export are at the origin of elevated concentrations of N_2O in the subsurface. N_2O is quickly outgassed to the atmosphere, leading to such areas of high N_2O emissions in the model.

Model-data discrepancies can be seen as a function of latitude in Figure 1d. The modeled N_2O flux maxima peak at around 40°S, i.e., around 10° north to that estimated by Nevison et al. (2004), although Southern Ocean data must be interpreted with caution. In the northern hemisphere the stripe in the North Pacific in not captured by the model, splitting the flux from the 45°N band into two peaks at 38°N and 55°N

3.2 Contemporary N_2O concentrations and the relationship to O_2

The model results at present day were evaluated against the MEMENTO database (Bange et al., 2009), which contains about 25,000 measurements of co-located N_2O and dissolved O_2 concentrations. Table 1 summarizes the standard deviation and correlation coefficients for P.TEMP and P.OMZ compared to MEMENTO. The standard deviation of the model output is very similar to MEMENTO, i.e., around 16 nmol L^{-1} of N_2O. However, the correlation coefficients between the sampled data points from MEMENTO and P.TEMP / P.OMZ are 0.49 and 0.42 respectively. Largest

discrepancies are found mostly in the deep ocean and in the OMZs.

Figure 2 compares the global average vertical profile of the observed N_2O against the results from the two parameterisations. The in-situ observations show three characteristic layers: the upper 100m layer with low (~10 nmol L^{-1}) N_2O concentration due to gas exchange keeping N_2O close to its saturation concentration, the mesopelagic layer, between 100 and 1500m, where N_2O is enriched via nitrification and denitrification in the OMZs, and the deep ocean beyond 1500m, with a relatively constant concentration of 18 nmol L^{-1} on average. Both parameterizations underestimate the N_2O concentration in the upper 100 meters, where most of the N_2O is potentially outgassed to the atmosphere. In the second layer, P.OMZ shows a fairly good agreement with the observations in the 500 to 900m band, whereas P.TEMP is too low by ~10 nmol L^{-1}. Below 1500m, both parameterizations simulate too high N_2O compared to the observations. This may be caused by the lack or underestimation of a sink process in the deep ocean, or by the too high concentrations used to initialize the model, which persist due to the rather short spin-up time of only 150 yrs.

The analysis of the model simulated N_2O concentrations as a function of model simulated O_2 shows the differences between the two parameterizations more clearly (Fig. 3a and 3b). Such a plot allows us to assess the model performance with regard to N_2O (Jin and Gruber, 2003), without being subject to the strong potential biases introduced by the model's deficiencies in simulating the distribution of O_2. This is particularly critical in the OMZs, where all models exhibit strong biases (Cocco et al., 2012; Bopp et al., 2013) (see also Fig. 3c). P.TEMP (Fig. 3a) slightly overestimates N_2O for dissolved O_2 concentrations above 100 µmol L^{-1}, and does not fully reproduce either the high N_2O values in the OMZs or the N_2O depletion when O_2 is almost completely consumed. P.OMZ (Figure 3b) overestimates the N_2O concentration over the whole range of O_2, with particularly high values of N_2O above 100 nmol L^{-1} due to the exponential function used in the OMZs. There, the observations suggest concentrations below 80 nmol L^{-1} for the same low O_2 values, consistent with the linear trend observed for higher O_2, which seems to govern over most of the O_2 spectrum, as suggested by Zamora et al. (2012). The discrepancy at low O_2 concentration may also stem from our choice of a too low N_2O consumption rate under essentially anoxic conditions. Finally, it should be considered that most of the MEMENTO data points are from OMZs and therefore N_2O

372 measurements could be biased towards higher values than the actual open ocean average,
373 where our model performs better.
374
375 4. Future oceanic N_2O
376
377 4.1 N_2O sea-to-air flux
378
379 The global oceanic N_2O emissions decrease relatively little over the next century (Fig. 4a)
380 between 4% and 12%. Namely, in P.TEMP, the emissions decrease by 0.15 TgN yr^{-1}
381 from 3.71 TgN yr^{-1} in 1985-2005 to 3.56 TgN yr^{-1} in 2080-2100 and in P.OMZ, the
382 decrease is slightly larger at 12%, i.e., amounting to 0.49 Tg N yr^{-1} from 4.03 to 3.54
383 TgN yr^{-1}. Notable is also the presence of a negative trend in N_2O emissions over the 20th
384 century, most pronounced in the P.OMZ parameterization. Considering the change over
385 the 20th and 21st centuries together, the model projects a decrease between 7 and 15%.
386 These relatively small global decreases mask more substantial changes at the regional scale,
387 with a mosaic of regions experiencing a substantial increase and regions experiencing a
388 substantial decrease (Fig. 4b and 4c). In both parameterizations, the oceanic N_2O
389 emissions decrease in the northern and south western oceanic basins (e.g., the North
390 Atlantic and Arabian Sea), by up to 25 mgN $m^{-2}yr^{-1}$. In contrast, the fluxes are simulated
391 to increase in the Eastern Tropical Pacific and in the Bay of Bengal. For the Benguela
392 Upwelling System (BUS) and the North Atlantic a bi-modal pattern emerges in 2100. As
393 was the case for the present-day distribution of the N_2O fluxes, the overall similarity
394 between the two parameterizations is a consequence of the dominance of the nitrification
395 (high-O_2) pathway in both parameterizations.
396 Nevertheless there are two regions where more substantial differences between the two
397 parameterizations emerge: the region overlying the oceanic OMZ at the BUS and the
398 Southern Ocean. In particular, the P.TEMP parameterization projects a larger
399 enhancement of the flux than P.OMZ at the BUS, whereas the emissions in the Southern
400 Ocean are enhanced in the P.OMZ parameterization.
401
402 4.2 Drivers of changes in N_2O emissions
403

Jorge 5/8/15 8:28 PM
Deleted: the

Jorge 5/8/15 8:29 PM
Deleted: s

Jorge 5/8/15 8:28 PM
Deleted: increase

Jorge 5/8/15 8:29 PM
Deleted: to

408 The changes in N_2O emissions may stem from a change in net N_2O production, a change
409 in the transport of N_2O from its location of production to the surface, or any
410 combination of the two, which includes also changes in N_2O storage. Next we determine
411 the contribution of these mechanisms to the overall decrease in N_2O emissions that our
412 model simulated for the 21st century.
413
414 4.2.1 Changes in N_2O production
415
416 In both parameterizations, global N_2O production is simulated to decrease over the 21st
417 century. The total N_2O production in P.OMZ decreases by 0.41 TgN yr^{-1} in 2080-2100
418 compared to the mean value over 1985-2005 (Fig. 5a). The parameterization P.OMZ
419 allows to isolate the contributions of high- and low-O_2 and will be analysed in greater
420 detail in the following sections. N_2O production via the high-O_2 pathway in P.OMZ
421 decreases in the same order than total production, by 0.35 TgN yr^{-1} in 2080-2100
422 compared to present. The N_2O production in the low-O_2 regions remains almost
423 constant across the experiment. In P.TEMP parameterization, the reduction in N_2O
424 production is much weaker than in P.OMZ due to the effect of the increasing
425 temperature. N_2O production decreases by 0.07 TgN yr^{-1} in 2080-2100 compared to
426 present (Fig. 5b).
427 The vast majority of the changes in the N_2O production in the P.OMZ parameterization
428 is caused by the high-O_2 pathway with virtually no contribution from the low-O_2
429 pathway (Fig. 5a). As the N_2O production in P.OMZ parameterization is solely driven
430 by changes in the O_2 consumption (Eq. (2)), which in our model is directly linked to
431 export production, the dominance of this pathway implies that primary driver for the
432 future changes in N_2O production in our model is the decrease in export of organic
433 matter (CEX). It was simulated to decrease by 0.97 PgC yr^{-1} in 2100, and the high degree
434 of correspondence in the temporal evolution of export and N_2O production in Fig. 5a
435 confirms this conclusion.
436 The close connection between N_2O production associated with the high-O_2 pathway and
437 changes in export production is also seen spatially (Fig. 5c), where the spatial pattern of
438 changes in export and changes in N_2O production are extremely highly correlated (shown
439 by stippling). Most of the small deviations are caused by lateral advection of organic

carbon, causing a spatial separation between changes in O_2 consumption and changes in organic matter export.

As there is an almost ubiquitous decrease of export in all of the major oceanic basins except at high latitudes, N_2O production decreases overall as well. Hotspots of reductions exceeding -10 mgN $m^{-2}yr^{-1}$ are found in the North Atlantic, the western Pacific and Indian basins (Fig. 5c). The fewer places where export increases, are also the locations of enhanced N_2O production. For example, a moderate increase of 3 mgN m^{-2} yr^{-1} is projected in the Southern Ocean, South Atlantic and Eastern Tropical Pacific. The general pattern of export changes, i.e., decreases in lower latitudes, increase in higher latitudes, is consistent generally with other model projection patterns (Bopp et al., 2013), although there exist very strong model-to-model differences at the more regional scale.

Although the global contribution of the changes in the low-O_2 N_2O production is small, this is the result of regionally compensating trends. In the model's OMZs, i.e., in the Eastern Tropical Pacific and in the Bay of Bengal, a significant increase in N_2O production is simulated in these locations (Fig. 5d), with an increase of more than 15 mgN m^{-2} yr^{-1}. This increase is primarily driven by the expansion of the OMZs in our model (shown by stippling), while changes in export contribute less. In effect, NEMO-PISCES projects a 20% increase in the hypoxic volume globally, from 10.2 to 12.3 x 10^6 km^3, and an increase in the suboxic volume from 1.1 to 1.6 x 10^6 km^3 in 2100 (Fig. 5e). Elsewhere, the changes in the N_2O production through the low-O_2 pathway are dominated by the changes in export, thus following the pattern of the changes seen in the high-O_2 pathway. Overall these changes are negative, and happen to nearly completely compensate the increase in production in the OMZs, resulting in the near constant global N_2O production by the low-O_2 production pathway up to year 2100.

4.2.2 Changes in storage of N_2O

A steady increase in the N_2O inventory is observed from present to 2100. The pool of oceanic N_2O down to 1500m, i.e., potentially outgassed to the atmosphere, increases by 8.9 TgN from 1985-2005 to year 2100 in P.OMZ, whereas P.TEMP is less sensitive to changes with an increase of 4.0 TgN on the time period considered (Fig. 6a). The inventory in the upper 1500m in P.OMZ is 237.0 TgN at present, while in P.TEMP in

the same depth band is 179.8 TgN. This means that the projected changes in the inventory represent an increase of about 4% and 2% in P.OMZ and P.TEMP respectively.

This increase in storage of N_2O in the ocean interior shows an homogeneous pattern for P.TEMP, with particular hotspots in the North Pacific, North Atlantic and the eastern boundary currents in the Pacific (Fig. 6b). The spatial variability is more pronounced in P.OMZ (Fig. 6c), related in part to the enhanced production associated with OMZs. Most of the projected changes in storage are associated with shoaling of the mixed layer depth (shown by stippling), suggesting that increase in N_2O inventories is caused by increased ocean stratification. Enhanced ocean stratification, in turn, occurs in response to increasing sea surface temperatures associated with global warming (Sarmiento et al., 2004).

4.2.3 Effects of the combined mechanisms on N_2O emissions

The drivers of the future evolution of oceanic N_2O emissions emerge from the preceding analysis. Firstly, a decrease in the high-O_2 production pathway driven by a reduced organic matter remineralization reduces N_2O concentrations below the euphotic zone. Secondly, the increased N_2O inventory at depth is caused by increased stratification and therefore to a less efficient transport to the sea-to-air interface, leading to a smaller N_2O flux.

The global changes in N_2O flux, N_2O production and N_2O storage for P.OMZ are presented in Fig. 7. Changes in N_2O flux and N_2O production are mostly of the same sign in almost all of the oceanic regions in line with the assumption of nitrification begin the dominant contribution to N_2O production. Changes in N_2O production in the subsurface are translated into corresponding changes in N_2O flux. There is only one oceanic region (Sub-Polar Pacific) where this correlation does not occur. N_2O inventory increases in all of the oceanic regions. The increase in inventory is particularly pronounced at low latitudes along the eastern boundary currents in the Equatorial and Tropical Pacific, Indian Ocean and also in smaller quantities in the Atlantic Ocean. Figure 7 shows how the decrease in N_2O production and increase in N_2O storage occurs in all oceanic basins.

Jorge 5/8/15 8:33 PM
Deleted: less

Jorge 5/8/15 8:04 PM
Deleted: The synergy among the driving mechanisms can be explored with a box model pursuing two objectives. First, to separate the effect of physical (i.e., increased stratification) and the biogeochemical (i.e., reduction of N_2O production in the high-O_2 regions) mechanisms on N_2O emissions. In this way we can reproduce future projections assuming that the only mechanisms ruling the N_2O dynamics in the future were those that we have proposed in our hypothesis, i.e., increased stratification and reduction of N_2O production in high-O_2 regions. Secondly, to explore a wider range of values for both mixing (i.e., degree of stratification) and efficiency of N_2O production in high-O_2 conditions. In the particular NEMO-PISCES model projection we have studied, changes in mixing and export are unique and can not be explored individually.
... [1]

5. Caveats in estimating N_2O using ocean biogeochemical models

The state variables upon which representation of N_2O in models rely, i.e., oxygen and export of carbon, are compared to the CMIP5 model ensemble to put our analysis in context of the current state-of-the-art model capabilities. We focus here our analysis on suboxic waters ($O_2 < 5$ µmol L^{-1}) and on export production. Whereas CMIP5 models tend to have large volumes of O_2 concentrations in the suboxic regime, it is not the case for our NEMO-PISCES simulation, which clearly underestimates the volume of low-oxygen waters as compared to the oxygen corrected World Ocean Atlas 2005 (WOA2005*) (Bianchi et al., 2012). The fact that NEMO-PISCES forced by IPSL-CM5A-LR is highly oxygenated is confirmed by Figure 8, where the histogram of the full O_2 spectrum of WOA2005* and NEMO-PISCES is shown. The O_2 distribution in the model shows a deficient representation of the OMZs, with higher concentrations than those from observations. The rest of the O_2 spectrum is well represented in our model.

The O_2 distribution in the model (Fig. 9) shows a deficient representation of the OMZs, with higher concentrations than those from observations in WOA2005* and the other CMIP5 models. NEMO-PISCES is therefore biased towards the high O_2 production pathway of N_2O due to the modeled O_2 fields.

When turning to the export of organic matter, NEMO-PISCES is close to the CMIP5 average value of 6.9 PgC yr^{-1}. The overall distribution of export is also very similar to the CMIP5 model mean and both show smaller values than those from the data-based estimate of 9.84 PgC yr^{-1} from Dunne et al., 2007 (Fig. 9).

The uncertainties derived from present and future model projections can be estimated using the spread in the CMIP5 model projection of export of organic matter and assuming a linear response between nitrification (or export) and N_2O production in the subsurface, which is assumed to be quickly outgassed to the atmosphere. In NEMO-PISCES, a decrease in 13% in export leads to a maximum decrease in N_2O emissions of 12% in the P.OMZ scenario. Based on results by Bopp et al. (2013), changes in export of carbon span -7% to -18% in the CMIP5 model ensemble at the end of the 21st century and for RCP8.5. The spread would propagate to a similar range in projected N_2O emissions across the CMIP5 model ensemble. Applying these values to present N_2O

Jorge 5/8/15 8:04 PM
Deleted: 9

Jorge 5/8/15 8:04 PM
Deleted: 10

Jorge 5/8/15 8:03 PM
Deleted: 10

562 emissions of 3.6 TgN yr^{-1}, uncertainties are then bracketed between -0.25 and -0.65 TgN
563 yr^{-1}.

564 Regarding the low-O_2 pathway, a similar approach is not that straight forward. Zamora et
565 al., (2012) found that a linear relationship between AOU and N_2O production might
566 occur even at the OMZ of the ETP. Zamora et al. (2012) acknowledged the fact that the
567 MEMENTO database includes N_2O advected from other regions and that mixing could
568 play a relevant role, smoothing the fit between N_2O and AOU from exponential to linear.
569 However, Zamora et al. (2012) quoting Frame and Casciotti (2010), suggested that
570 regions were an exponential relationship in N_2O production is present might be rare, that
571 other non-exponential N_2O production processes might occur and therefore the plot they
572 presented could describe the actual linear relationship between N_2O production and
573 oxygen consumption. Based on this hypothesis, we could refer again to the linear
574 relationship suggested in the high-O_2 and export scenario. However, in this case the
575 CMIP5 model projections of changes in the hypoxic and suboxic volumes differ
576 substantially. Most models project an expansion of the OMZs in the +2% to +16% range
577 in the suboxic volume (O_2 < 5 µmol L^{-1}). There are, however, models that project a slight
578 reduction of 2%. Spatial variability of projections add to the spread between CMIP5
579 models. These discrepancies suggest that uncertainties from this spread must be
580 interpreted with caution when estimating potential future N_2O emissions.

581 The use of O_2 consumption as a proxy for the actual N_2O production plays therefore a
582 pivotal role in the uncertainties in N_2O model estimations. Future model development
583 should aim at the implementation of mechanistic parameterizations of N_2O production
584 based on nitrification and denitrification rates. Further, in order to determine accurate
585 O_2 boundaries for both N_2O production and N_2O consumption at the core of OMZs
586 additional measurements and microbial experiments are needed. The contribution of the
587 high-O_2 pathway that was considered in this model analysis might be a conservative
588 estimate. Freing et al. (2012) suggested that the high-O_2 pathway could be responsible of
589 93% of the total N_2O production. Assuming that changes in the N_2O flux are mostly
590 driven by N_2O production via nitrification, that would suggest a larger reduction in the
591 marine N_2O emissions in the future. However, the mismatch between NEMO-PISCES
592 and the Nevison et al. (2004) spatial distribution of N_2O emissions in the western part of
593 the basins suggests that changes in the future might not be as big as those projected in the

model in such regions. Changes would be then distributed more homogeneously.

The model assumption neglecting N_2O production in the upper 100m avoids one important source of uncertainty in estimating global oceanic N_2O fluxes. In case nitrification occurs in the euphotic layer, our results would be facing a significant uncertainty of at least ±25% in N_2O emissions according to Zamora and Oschlies (2014) analysis using the UVic Earth System Climate Model. Finally, Zamora et al. (2012) observed a higher than expected N_2O consumption at the core of the OMZ in the Eastern Tropical Pacific, occurring at an upper threshold of 10 μmol L^{-1}. The contribution of OMZs to total N_2O production remains an open question. N_2O formation associated with OMZs might be counterbalanced by its own local consumption, leading to the attenuation of the only increasing source of N_2O attributable to the projected future expansion of OMZs (Steinacher et al., 2010; Bopp et al., 2013).

The combined effect of climate change and ocean acidification has not been analyzed in this study. N_2O production processes might be altered by the response of nitrification to increasing levels of seawater pCO_2 (Huesemann et al., 2002; Beman et al. 2011). Beman et al. (2011) reported a reduction in nitrification in response to decreasing pH. This result suggests that N_2O production might decrease beyond what we have estimated only due to climate change. Conversely, negative changes in the ballast effect could potentially reinforce nitrification at shallow depth in response to less efficient POC export to depth and shallow remineralization (Gehlen et al., 2011). Regarding N_2O formation via denitrification, changes in seawater pH as a consequence of higher levels of CO_2 might not be substantial enough to change the N_2O production efficiency, assuming a similar response of marine denitrifiers as reported for denitrifying bacteria have in terrestrial systems (Liu et al., 2010). Finally, the C:N ratio in export production (Riebesell et al., 2007) might increase in response to ocean acidification, potentially leading to a greater expansion of OMZs than simulated here (Oschlies et al., 2008; Tagliabue et al., 2011), and therefore to enhanced N_2O production associated with the low-O_2 pathway.

Changes in atmospheric nitrogen deposition have not been considered in this study. It has been suggested that due to anthropogenic activities the additional amount of reactive nitrogen in the ocean could fuel primary productivity and N_2O production. Estimates are however low, around 3-4% of the total oceanic emissions (Suntharalingam et al., 2012).

Longer simulation periods could reveal additional effects on N_2O transport beyond changes in upwelling or meridional transport of N_2O in the subsurface (Suntharalingam and Sarmiento, 2000) that have been observed in this transient simulation. Long-term responses might include eventual ventilation of the N_2O reservoir in the Southern Ocean, highlighting the role of upwelling regions as an important source of N_2O when longer time periods are considered in model projections. Additional studies using other ocean biogeochemical models might also yield alternative values using the same parameterizations. N_2O production is particularly sensitive to the distribution and magnitude of export of organic matter and O_2 fields defined in models.

6. Contribution of future N_2O to climate feedbacks

Changes in the oceanic emissions of N_2O to the atmosphere will have an impact on atmospheric radiative forcing, with potential feedbacks on the climate system. Based on the estimated 4 to 12% decrease in N_2O sea-to-air flux over the 21st century under RCP8.5, we estimated the feedback factor for these changes as defined by Xu-Ri et al. (2012). Considering the reference value of the pre-industrial atmospheric N_2O concentration of 280 ppb in equilibrium, and its associated global N_2O emissions of 11.8 TgN yr^{-1}, we quantify the resulting changes in N_2O concentration per degree for the two projected emissions in 2100 using P.TEMP and P.OMZ. The model projects changes in N_2O emissions of -0.16 and -0.48 TgN yr^{-1} respectively, whereas surface temperature is assumed to increase globally by 3°C on average according to the physical forcing used in our simulations. These results yield -0.05 and -0.16 TgN yr^{-1} K^{-1}, or alternatively -1.25 and -3.80 ppb K^{-1} for P.TEMP and P.OMZ respectively. Using Joos et al. (2001) we calculate the feedback factor in equilibrium for projected changes in emissions to be -0.005 and -0.014 W $m^{-2}K^{-1}$ in P.TEMP and P.OMZ.

Stocker et al. (2013) projected changes in terrestrial N_2O emissions in 2100 using transient model simulations leading to feedback strengths between +0.001 and +0.015 W $m^{-2}K^{-1}$. Feedback strengths associated with the projected decrease of oceanic N_2O emissions are of the same order of magnitude as those attributable to changes in the terrestrial sources of N_2O, yet opposite in sign, suggesting a compensation of changes in radiative forcing due to future increasing terrestrial N_2O emissions. At this stage,

potential compensation between land and ocean emissions is to be taken with caution, as it relies of a single model run with constant atmospheric N_2O.

7. Conclusions

Our simulations suggest that anthropogenic climate change could lead to a global decrease in oceanic N_2O emissions during the 21st century. This maximum projected decrease of 12% in marine N_2O emissions for the business-as-usual high CO_2 emissions scenario would compensate for the estimated increase in N_2O fluxes from the terrestrial biosphere in response to anthropogenic climate change (Stocker et al. 2013), so that the climate-N_2O feedback may be more or less neutral over the coming decades.

The main mechanisms contributing to the reduction of marine N_2O emissions are a decrease in N_2O production in high oxygenated waters as well as an increase in ocean vertical stratification that acts to decrease the transport of N_2O from the sub-surface to the surface ocean. Despite the decrease in both N_2O production and N_2O emissions, simulations suggest that the global marine N_2O inventory may increase from 2005 to 2100. This increase is explained by the reduced transport of N_2O from the production zones to the air-sea interface.

Differences between the two parameterizations used here are more related to biogeochemistry rather than changes in ocean circulation. Despite sharing the high-O_2 N_2O production pathway, leading to a decrease in N_2O emissions in both cases, the role of warming in P.TEMP or higher N_2O yields at low-O_2 concentrations in P.OMZ translate into notable differences in the evolution of the two production pathways. However, the dominant effect of changes in stratification in both parameterizations drives ultimately the homogeneous response of the parameterizations considered in model projections in the next century.

The N_2O production pathways demand however a better understanding in order to enable an improved representation of processes in models. At a first order, the efficiencies of the production processes in response to higher temperatures or increased seawater pCO_2 are required. Second order effects such as changes in the O_2 boundaries at which nitrification and denitrification occur must be also taken into account. In the absence of process-based parameterizations, N_2O production parameterizations will still rely on

690 export of organic carbon and oxygen levels. Both need to be improved in global
691 biogeochemical models.
692 The same combination of mechanisms (i.e., change in export production and ocean
693 stratification) have been identified as drivers of changes in oceanic N_2O emissions during
694 the Younger Dryas by Goldstein et al. (2003). The N_2O flux decreased, while the N_2O
695 reservoir was fueled by longer residence times of N_2O caused by increased stratification.
696 Other studies point towards changes in the N_2O production at the OMZs as the main
697 reason for variations in N_2O observed in the past (Suthhof et al., 2001). Whether these
698 mechanisms are plausible drivers of changes beyond year 2100 remains an open question
699 that needs to be addressed with longer simulations.
700

8. Acknowledgements

We thank Cynthia Nevison for providing us the N_2O sea-to-air flux dataset. We thank Annette Kock and Herman Bange for the availability of the MEMENTO database (https://memento.geomar.de). We thank Christian Ethé for help analyzing PISCES model drift. Comments by Parvadha Suntharalingam and three anonymous reviewers improved significantly this manuscript. Nicolas Gruber acknowledges the support of ETH Zürich. This work has been supported by the European Union via the Greencycles II FP7-PEOPLE-ITN-2008, number 238366.

710 7. References
711
712 Aumont, O., and Bopp, L.: Globalizing results from ocean in situ iron fertilization studies,
713 Global Biogeochemical Cycles, GB2017, 20, 10.1029/2005gb002591, 2006.
714 Bange, H. W., Rixen, T., Johansen, A. M., Siefert, R. L., Ramesh, R., Ittekkot, V., Hoffmann,
715 M. R., and Andreae, M. O.: A revised nitrogen budget for the Arabian Sea, Global
716 Biogeochemical Cycles, 14, 1283-1297, 10.1029/1999gb001228, 2000.
717 Bange, H. W., Bell, T. G., Cornejo, M., Freing, A., Uher, G., Upstill-Goddard, R. C., and
718 Zhang, G.: MEMENTO: a proposal to develop a database of marine nitrous oxide and methane
719 measurements, Environmental Chemistry, 6, 195-197, 10.1071/en09033, 2009.
720 Beman, J. M., Chow, C.-E., King, A. L., Feng, Y., Fuhrman, J. A., Andersson, A., Bates, N. R.,
721 Popp, B. N., and Hutchins, D. A.: Global declines in oceanic nitrification rates as a consequence
722 of ocean acidification, Proceedings of the National Academy of Sciences of the United States of
723 America, 108, 208-213, 10.1073/pnas.1011053108, 2011.
724 Bianchi, D., Dunne, J. P., Sarmiento, J. L., and Galbraith, E. D.: Data-based estimates of
725 suboxia, denitrification, and N2O production in the ocean and their sensitivities to dissolved O-
726 2, Global Biogeochemical Cycles, 26, GB2009, 10.1029/2011gb004209, 2012.
727 Bindoff, N., Willebrand, J., Artale, V., Cazenave, A., Gregory, J., Gulev, S., Hanawa, K.,
728 Le Quere, C., Levitus, S., Norjiri, Y., Shum, C., Talley, L., and Unnikrishnan, A.:
729 Observations: Oceanic Climate Change and Sea Level, In Climate Change 2007: The
730 Physical Science Basis.Contribution of Working Group I to the Fourth Assessment
731 Report of the Intergovernmental Panel on Climate Change, 2007.
732 Bopp, L., Resplandy, L., Orr, J. C., Doney, S. C., Dunne, J. P., Gehlen, M., Halloran, P.,
733 Heinze, C., Ilyina, T., Seferian, R., Tjiputra, J., and Vichi, M.: Multiple stressors of ocean
734 ecosystems in the 21st century: projections with CMIP5 models, Biogeosciences, 10, 6225-6245,
735 10.5194/bg-10-6225-2013, 2013.
736 Butler, J. H., Elkins, J. W., Thompson, T. M., and Egan, K. B.: Tropospheric and dissolved
737 N_2O of the west pacific and east-indian oceans during the el-nino southern oscillation event of
738 1987, Journal of Geophysical Research-Atmospheres, 94, 14865-14877,
739 10.1029/JD094iD12p14865, 1989.
740 Ciais, P., Sabine, C., Bala, G., Bopp, L., Brovkin, V., Canadell, J., Chhabra, A., DeFries,
741 R., Galloway, J., Heimann, M., Jones, C., Le Quéré, C., Myneni, RB., Piao, S. and

742 Thornton, P.: Carbon and Other Biogeochemical Cycles. In: Climate Change 2013: The
743 Physical Science Basis. Contribution of Working Group I to the Fifth Assessment Report
744 of the Intergovernmental Panel on Climate Change, 2013.
745 Cocco, V., Joos, F., Steinacher, M., Froelicher, T. L., Bopp, L., Dunne, J., Gehlen, M., Heinze,
746 C., Orr, J., Oschlies, A., Schneider, B., Segschneider, J., and Tjiputra, J.: Oxygen and indicators
747 of stress for marine life in multi-model global warming projections, Biogeosciences, 10, 1849-
748 1868, 10.5194/bg-10-1849-2013, 2013.
749 Cohen, Y., and Gordon, L. I.: Nitrous-oxide in oxygen minimum of eastern tropical north
750 pacific - evidence for its consumption during denitrification and possible mechanisms for its
751 production, Deep-Sea Research, 25, 509-524, 10.1016/0146-6291(78)90640-9, 1978.
752 Cohen, Y., and Gordon, L. I.: Nitrous-oxide production in the ocean, Journal of Geophysical
753 Research-Oceans and Atmospheres, 84, 347-353, 10.1029/JC084iC01p00347, 1979.
754 Crutzen, P. J.: Influence of nitrogen oxides on atmospheric ozone content, Quarterly Journal of
755 the Royal Meteorological Society, 96, 320-326, 10.1002/qj.49709640815, 1970.
756 de Wilde, H. P. J., and de Bie, M. J. M.: Nitrous oxide in the Schelde estuary: production by
757 nitrification and emission to the atmosphere, Marine Chemistry, 69, 203-216, 10.1016/s0304-
758 4203(99)00106-1, 2000.
759 Deutsch, C., Brix, H., Ito, T., Frenzel, H., and Thompson, L.: Climate-Forced Variability of
760 Ocean Hypoxia, Science, 333, 336-339, 10.1126/science.1202422, 2011.
761 Dufresne, J. L., Foujols, M. A., Denvil, S., Caubel, A., Marti, O., Aumont, O., Balkanski, Y.,
762 Bekki, S., Bellenger, H., Benshila, R., Bony, S., Bopp, L., Braconnot, P., Brockmann, P.,
763 Cadule, P., Cheruy, F., Codron, F., Cozic, A., Cugnet, D., de Noblet, N., Duvel, J. P., Ethe, C.,
764 Fairhead, L., Fichefet, T., Flavoni, S., Friedlingstein, P., Grandpeix, J. Y., Guez, L., Guilyardi,
765 E., Hauglustaine, D., Hourdin, F., Idelkadi, A., Ghattas, J., Joussaume, S., Kageyama, M.,
766 Krinner, G., Labetoulle, S., Lahellec, A., Lefebvre, M. P., Lefevre, F., Levy, C., Li, Z. X., Lloyd,
767 J., Lott, F., Madec, G., Mancip, M., Marchand, M., Masson, S., Meurdesoif, Y., Mignot, J.,
768 Musat, I., Parouty, S., Polcher, J., Rio, C., Schulz, M., Swingedouw, D., Szopa, S., Talandier,
769 C., Terray, P., Viovy, N., and Vuichard, N.: Climate change projections using the IPSL-CM5
770 Earth System Model: from CMIP3 to CMIP5, Climate Dynamics, 40, 2123-2165,
771 10.1007/s00382-012-1636-1, 2013.
772 Dunne, J. P., Sarmiento, J. L., and Gnanadesikan, A.: A synthesis of global particle export
773 from the surface ocean and cycling through the ocean interior and on the seafloor, Global

774 Biogeochemical Cycles, 21, GB4006,10.1029/2006gb002907, 2007.
775 Elkins, J. W., Wofsy, S. C., McElroy, M. B., Kolb, C. E., and Kaplan, W. A.: Aquatic sources
776 and sinks for nitrous-oxide, Nature, 275, 602-606, 10.1038/275602a0, 1978.
777 Farias, L., Paulmier, A., and Gallegos, M.: Nitrous oxide and N-nutrient cycling in the
778 oxygen minimum zone off northern Chile, Deep-Sea Research Part I-Oceanographic
779 Research Papers, 54, 164-180, 10.1016/j.dsr.2006.11.003, 2007.
780 Fletcher, S. E. M., Gruber, N., Jacobson, A. R., Gloor, M., Doney, S. C., Dutkiewicz, S.,
781 Gerber, M., Follows, M., Joos, F., Lindsay, K., Menemenlis, D., Mouchet, A., Muller, S. A.,
782 and Sarmiento, J. L.: Inverse estimates of the oceanic sources and sinks of natural CO_2 and
783 the implied oceanic carbon transport, Global Biogeochemical Cycles, 21, GB1010,
784 10.1029/2006gb002751, 2007.
785 Frame, C. H., and Casciotti, K. L.: Biogeochemical controls and isotopic signatures of nitrous
786 oxide production by a marine ammonia-oxidizing bacterium, Biogeosciences, 7, 2695-2709,
787 10.5194/bg-7-2695-2010, 2010.
788 Freing, A., Wallace, D. W. R., Tanhua, T., Walter, S., and Bange, H. W.: North Atlantic
789 production of nitrous oxide in the context of changing atmospheric levels, Global
790 Biogeochemical Cycles, 23, GB4015, 10.1029/2009gb003472, 2009.
791 Freing, A., Wallace, D. W. R., and Bange, H. W.: Global oceanic production of nitrous oxide,
792 Philosophical Transactions of the Royal Society B-Biological Sciences, 367, 1245-1255,
793 10.1098/rstb.2011.0360, 2012.
794 Gehlen, M., Gruber, N., Gangstø, R., Bopp, L., and Oschlies, A.: Biogeochemical consequences
795 of ocean acidification and feedbacks to the earth system. Ocean acidification: 230-248, 2011.
796 Goldstein, B., Joos, F., and Stocker, T. F.: A modeling study of oceanic nitrous oxide during the
797 Younger Dryas cold period, Geophysical Research Letters, 30, 1092, 10.1029/2002gl016418,
798 2003.
799 Goreau, T. J., Kaplan, W. A., Wofsy, S. C., McElroy, M. B., Valois, F. W., and Watson, S. W.:
800 Production of NO_2^- and N_2O by nitrifying bacteria at reduced concentrations of oxygen, Applied
801 and Environmental Microbiology, 40, 526-532, 1980.
802 Gruber, N., and Galloway, J. N.: An Earth-system perspective of the global nitrogen cycle,
803 Nature, 451, 293-296, 10.1038/nature06592, 2008.
804 Gruber, N.: Warming up, turning sour, losing breath: ocean biogeochemistry under global
805 change, Philosophical Transactions of the Royal Society a-Mathematical Physical and
806 Engineering Sciences, 369, 1980-1996, 10.1098/rsta.2011.0003, 2011.

Gruber, N.: The marine nitrogen cycle: Overview of distributions and processes. In: Nitrogen in the marine environment, 2nd edition, 1-50, 2008.

Huesemann, M. H., Skillman, A. D., and Crecelius, E. A.: The inhibition of marine nitrification by ocean disposal of carbon dioxide, Marine Pollution Bulletin, 44, 142-148, 10.1016/s0025-326x(01)00194-1, 2002.

Jin, X., and Gruber, N.: Offsetting the radiative benefit of ocean iron fertilization by enhancing N_2O emissions, Geophysical Research Letters, 30, 2249, 10.1029/2003gl018458, 2003.

Johnston, H.: Reduction of stratospheric ozone by nitrogen oxide catalysts from supersonic transport exhaust, Science, 173, 517-522, 10.1126/science.173.3996.517, 1971.

Joos, F., Prentice, I. C., Sitch, S., Meyer, R., Hooss, G., Plattner, G. K., Gerber, S., and Hasselmann, K.: Global warming feedbacks on terrestrial carbon uptake under the Intergovernmental Panel on Climate Change (IPCC) emission scenarios, Global Biogeochemical Cycles, 15, 891-907, 10.1029/2000gb001375, 2001.

Keeling, R. F., Koertzinger, A., and Gruber, N.: Ocean Deoxygenation in a Warming World, Annual Review of Marine Science, 2, 199-229, 10.1146/annurev.marine.010908.163855, 2010.

Liu, B., Morkved, P. T., Frostegard, A., and Bakken, L. R.: Denitrification gene pools, transcription and kinetics of NO, N_2O and N-2 production as affected by soil pH, Fems Microbiology Ecology, 72, 407-417, 10.1111/j.1574-6941.2010.00856.x, 2010.

Mantoura, R. F. C., Law, C. S., Owens, N. J. P., Burkill, P. H., Woodward, E. M. S., Howland, R. J. M., and Llewellyn, C. A.: Nitrogen biogeochemical cycling in the northwestern indian-ocean, Deep-Sea Research Part II-Topical Studies in Oceanography, 40, 651-671, 1993.

Myhre, G., Shindell, D., Bréon, F.-M., Collins, W., Fuglestvedt, J., Huang, J., Koch, D., Lamarque, J.-F., Lee, D., Mendoza, B., Nakajima, T., Robock, A., Stephens, G., Takemura, T. and Zhang, H.: Anthropogenic and Natural Radiative Forcing. In: Climate Change 2013: The Physical Science Basis. Contribution of Working Group I to the Fifth Assessment Report of the Intergovernmental Panel on Climate Change, 2013.

Nevison, C. D., Lueker, T. J., and Weiss, R. F.: Quantifying the nitrous oxide source from coastal upwelling, Global Biogeochemical Cycles, 18, GB1018, 10.1029/2003gb002110, 2004.

Nevison, C., Butler, J. H., and Elkins, J. W.: Global distribution of N_2O and the Delta N_2O-AOU yield in the subsurface ocean, Global Biogeochemical Cycles, 17, 1119, 10.1029/2003gb002068, 2003.

839 Nevison, C. D., Weiss, R. F., and Erickson, D. J.: Global oceanic emissions of nitrous-oxide,
840 Journal of Geophysical Research-Oceans, 100, 15809-15820, 10.1029/95jc00684, 1995.
841 Oschlies, A., Schulz, K. G., Riebesell, U., and Schmittner, A.: Simulated 21st century's increase
842 in oceanic suboxia by CO2-enhanced biotic carbon export, Global Biogeochemical Cycles, 22,
843 GB4008, 10.1029/2007gb003147, 2008.
844 Prather, M. J., Holmes, C. D., and Hsu, J.: Reactive greenhouse gas scenarios: Systematic
845 exploration of uncertainties and the role of atmospheric chemistry, Geophysical Research Letters,
846 39, L09803, 10.1029/2012gl051440, 2012.
847 Punshon, S., and Moore, R. M.: Nitrous oxide production and consumption in a eutrophic
848 coastal embayment, Marine Chemistry, 91, 37-51, 10.1016/j.marchem.2004.04.003, 2004.
849 Ravishankara, A. R., Daniel, J. S., and Portmann, R. W.: Nitrous Oxide (N2O): The Dominant
850 Ozone-Depleting Substance Emitted in the 21st Century, Science, 326, 123-125,
851 10.1126/science.1176985, 2009.
852 Resplandy, L., Levy, M., Bopp, L., Echevin, V., Pous, S., Sarma, V. V. S. S., and Kumar, D.:
853 Controlling factors of the oxygen balance in the Arabian Sea's OMZ, Biogeosciences, 9, 5095-
854 5109, 10.5194/bg-9-5095-2012, 2012.
855 Riebesell, U., Schulz, K. G., Bellerby, R. G. J., Botros, M., Fritsche, P., Meyerhoefer, M., Neill,
856 C., Nondal, G., Oschlies, A., Wohlers, J., and Zoellner, E.: Enhanced biological carbon
857 consumption in a high CO2 ocean, Nature, 450, 545-548, 10.1038/nature06267, 2007.
858 Sarmiento, J. L., Slater, R., Barber, R., Bopp, L., Doney, S. C., Hirst, A. C., Kleypas, J., Matear,
859 R., Mikolajewicz, U., Monfray, P., Soldatov, V., Spall, S. A., and Stouffer, R.: Response of ocean
860 ecosystems to climate warming, Global Biogeochemical Cycles, 18, GB3003,
861 10.1029/2003gb002134, 2004.
862 Steinacher, M., Joos, F., Frolicher, T. L., Bopp, L., Cadule, P., Cocco, V., Doney, S. C., Gehlen,
863 M., Lindsay, K., Moore, J. K., Schneider, B., and Segschneider, J.: Projected 21st century
864 decrease in marine productivity: a multi-model analysis, Biogeosciences, 7, 979-1005, 2010.
865 Stocker, B. D., Roth, R., Joos, F., Spahni, R., Steinacher, M., Zaehle, S., Bouwman, L., Xu, R.,
866 and Prentice, I. C.: Multiple greenhouse-gas feedbacks from the land biosphere under future
867 climate change scenarios, Nature Climate Change, 3, 666-672, 10.1038/nclimate1864, 2013.
868 Suntharalingam, P., and Sarmiento, J. L.: Factors governing the oceanic nitrous oxide
869 distribution: Simulations with an ocean general circulation model, Global Biogeochemical
870 Cycles, 14, 429-454, 10.1029/1999gb900032, 2000.

Suntharalingam, P., Sarmiento, J. L., and Toggweiler, J. R.: Global significance of nitrous-oxide production and transport from oceanic low-oxygen zones: A modeling study, Global Biogeochemical Cycles, 14, 1353-1370, 10.1029/1999gb900100, 2000.

Suntharalingam, P., Buitenhuis, E., Le Quere, C., Dentener, F., Nevison, C., Butler, J. H., Bange, H. W., and Forster, G.: Quantifying the impact of anthropogenic nitrogen deposition on oceanic nitrous oxide, Geophysical Research Letters, 39, L07605, 10.1029/2011gl050778, 2012.

Suthhof, A., Ittekkot, V., and Gaye-Haake, B.: Millennial-scale oscillation of denitrification intensity in the Arabian Sea during the late Quaternary and its potential influence on atmospheric N_2O and global climate, Global Biogeochemical Cycles, 15, 637-649, 10.1029/2000gb001337, 2001.

Tagliabue, A., Bopp, L., and Gehlen, M.: The response of marine carbon and nutrient cycles to ocean acidification: Large uncertainties related to phytoplankton physiological assumptions, Global Biogeochemical Cycles, 25, GB3017, 10.1029/2010gb003929, 2011.

Takahashi, T., Broecker, W. S., and Langer, S.: Redfield ratio based on chemical-data from isopycnal surfaces, Journal of Geophysical Research-Oceans, 90, 6907-6924, 10.1029/JC090iC04p06907, 1985.

Tiedje, J.M.: Ecology of denitrification and dissimilatory nitrate reduction to ammonium. Biology of anaerobic microorganisms, 179–244, 1988.

Wanninkhof, R.: Relationship between wind-speed and gas-exchange over the ocean, Journal of Geophysical Research-Oceans, 97, 7373-7382, 10.1029/92jc00188, 1992.

Weiss, R. F., and Price, B. A.: Nitrous-oxide solubility in water and seawater, Marine Chemistry, 8, 347-359, 10.1016/0304-4203(80)90024-9, 1980.

Westley, M. B., Yamagishi, H., Popp, B. N., and Yoshida, N.: Nitrous oxide cycling in the Black Sea inferred from stable isotope and isotopomer distributions, Deep-Sea Research Part Ii-Topical Studies in Oceanography, 53, 1802-1816, 10.1016/j.dsr2.2006.03.012, 2006.

Yoshida, N., Morimoto, H., Hirano, M., Koike, I., Matsuo, S., Wada, E., Saino, T., and Hattori, A.: Nitrification rates and N-15 abundances of N_2O and NO_3^- in the western north pacific, Nature, 342, 895-897, 10.1038/342895a0, 1989.

Zamora, L. M., and Oschlies, A.: Surface nitrification: A major uncertainty in marine N_2O emissions, Geophysical Research Letters, 41, 4247-4253, 10.1002/2014gl060556, 2014.

Zamora, L. M., Oschlies, A., Bange, H. W., Huebert, K. B., Craig, J. D., Kock, A., and Loescher, C. R.: Nitrous oxide dynamics in low oxygen regions of the Pacific: insights from the MEMENTO database, Biogeosciences, 9, 5007-5022, 10.5194/bg-9-5007-2012, 2012.

Zehr, J. P., and Ward, B. B.: Nitrogen cycling in the ocean: New perspectives on processes and paradigms, Applied and Environmental Microbiology, 68, 1015-1024, 10.1128/aem.68.3.1015-1024.2002, 2002.

908 Table 1: Standard deviation and correlation coefficients between P.TEMP and P.OMZ
909 parameterizations with respect to MEMENTO database observations (Bange et al., 2009).
910

	P.TEMP	P.OMZ	OBS
Standard deviation (in nmol N_2O L^{-1})	12	18	16
Correlation coefficient with obs.	0.49	0.42	-

911
912

913
914
915

Jorge 5/8/15 8:03 PM

Deleted: Page Break

Table S1: Box model boundary conditions and parameters. NEMO-PISCES model output values are taken from the historical averaged 1985 to 2005 time period and the future averaged 2080 to 2100 time period. ... [2]

Fig.1: N_2O sea-to-air flux (in mgN m^{-2} yr^{-1}) from (a) P.TEMP parameterzation averaged for the 1985 to 2005 time period in the historical simulation, (b) P.OMZ parameterization over the same time period, (c) data product of Nevison et al. (2004) and (d) latitudinal N_2O sea-to-air flux (in TgN $deg^{-1}yr^{-1}$) from Nevison et al. (2004) (black), P.TEMP (blue) and P.OMZ (red).

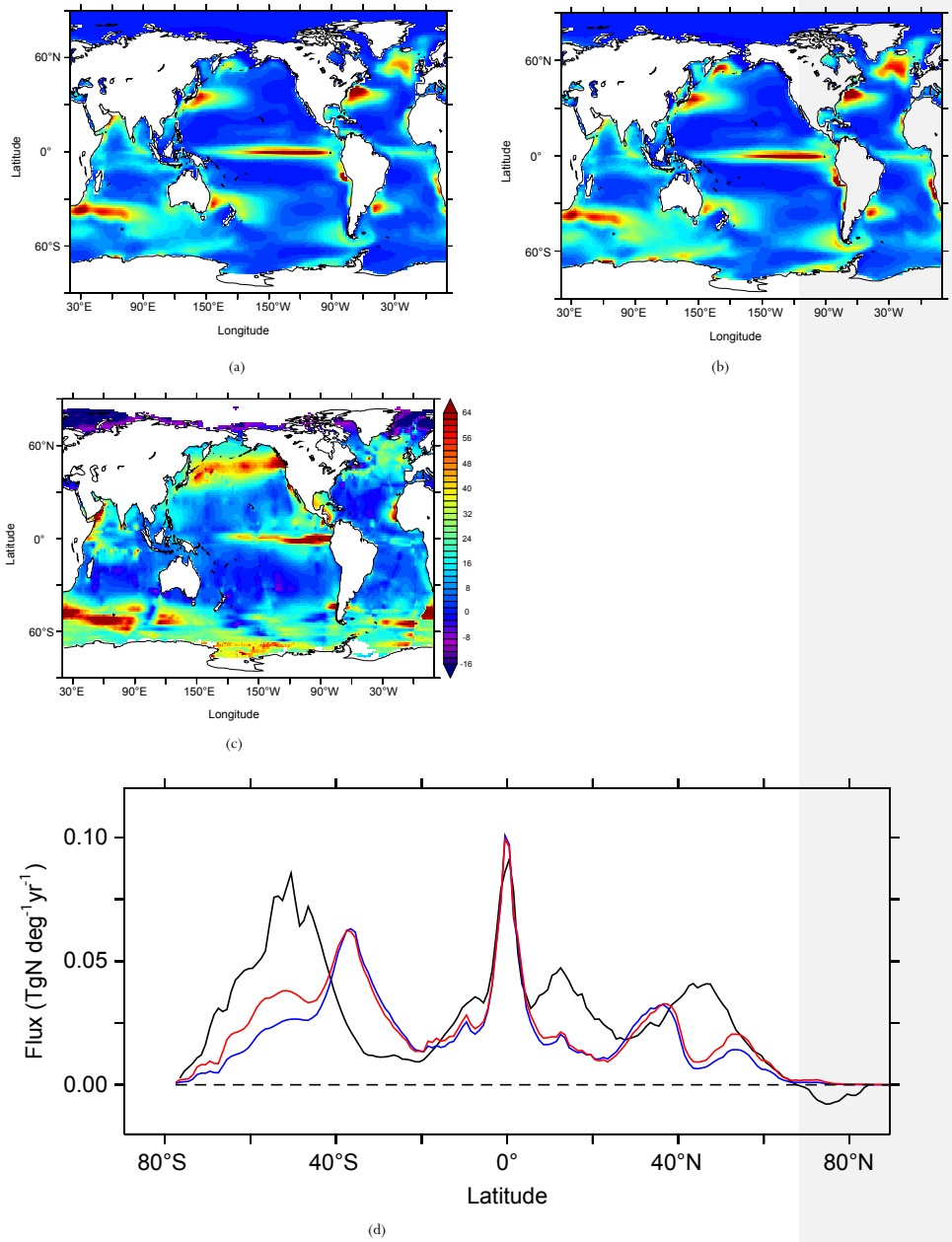

Fig.2: Global average depth profile of N_2O concentration (in nmol L^{-1}) from the MEMENTO database (dots) (Bange et al., 2009), P.TEMP (blue) and P.OMZ (red). Model parameterizations are averaged over the 1985 to 2005 time period from the historical simulation.

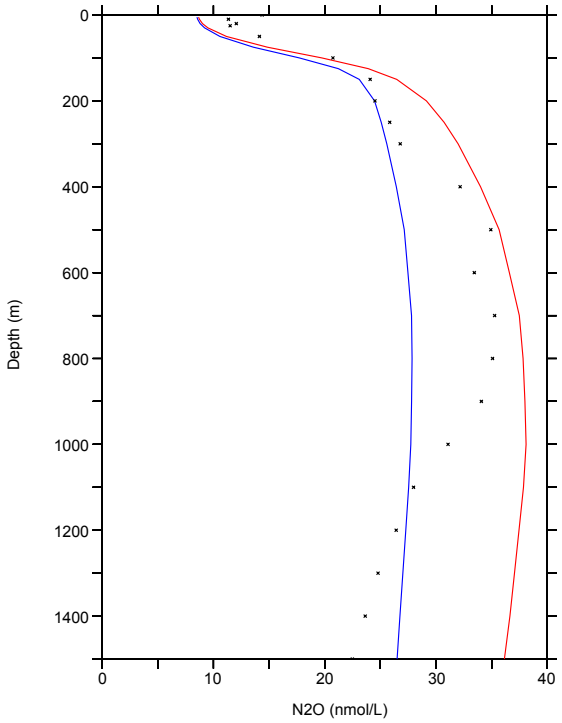

Fig. 3: Relationship between O_2 concentration (in µmol L^{-1}) and N_2O concentration (in nmol L^{-1}) in the MEMENTO database (black) (Bange et al., 2009), compared to model (a) P.TEMP (blue) and (b) P.OMZ (red) parameterizations averaged over the 1985 to 2005 time period from the historical simulation.

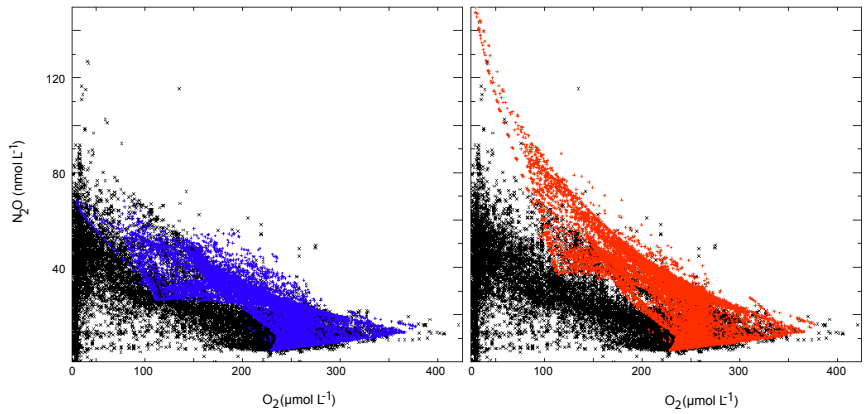

(a) (b)

Fig 4: (a) N_2O sea-to-air flux (in TgN yr^{-1}) from 1851 to 2100 in P.TEMP (blue) and P.OMZ (red) using the historical and future RCP8.5 simulations. Dashed lines indicate the mean value over the 1985 to 2005 time period. Change in N_2O sea-to-air flux (mgN $m^{-2}yr^{-1}$) from the averaged 2080-2100 to 1985-2005 time periods in future RCP8.5 and historical simulations in (b) P.TEMP and (c) P.OMZ parameterizations.

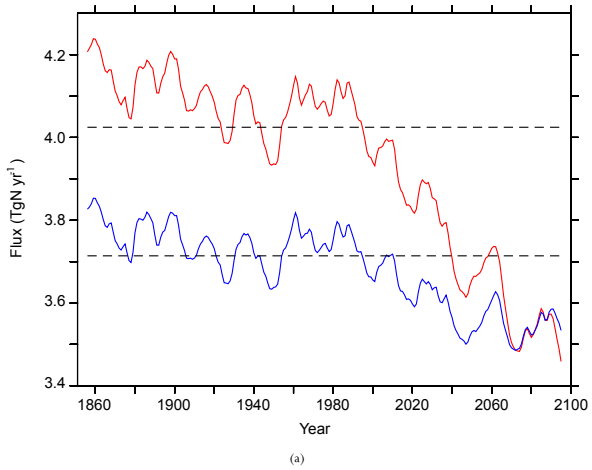

(a)

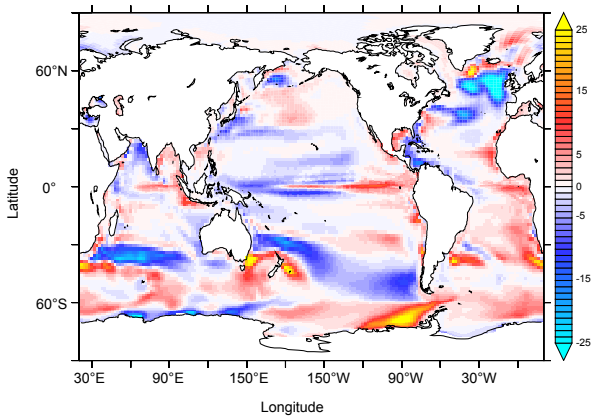

(b)

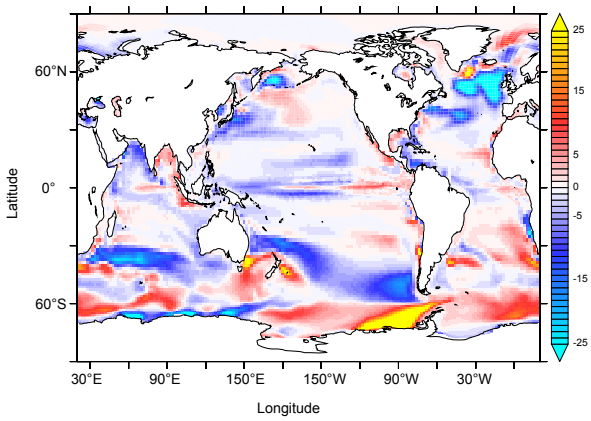
60°N
0°
60°S
Latitude
30°E
90°E
150°E
150°W
90°W
30°W
Longitude
25
15
5
0
-5
-15
-25

(c)

Fig 5: (a) Anomalies in export of organic matter at 100m (green), low-O_2 production pathway (short dashed red), high-O_2 production pathway (long dashed red) and total P.OMZ production (red) from 1851 to 2100 using the historical and future RCP8.5 simulations. (b) Anomalies in export of organic matter at 100m (green) and P.TEMP production (blue) over the same time period. (c) Change in high-O_2 production pathway of N_2O (in mgN m^{-2} yr^{-1}) in the upper 1500m between 2080-2100 to 1985-2005 averaged time periods. Hatched areas indicate regions where change in export of organic matter at 100m deep have the same sign as in changes in high-O_2 production pathway. (d) Change in low-O_2 production pathway of N_2O (in mgN m^{-2} yr^{-1}) in the upper 1500m between 2080-2100 to 1985-2005 averaged time periods. Hatched areas indicate regions where oxygen minimum zones (O_2 < 5 µmol L^{-1}) expand. (e) Volume (in 10^6 km^3) of hypoxic (black, O_2 < 60 µmol L^{-1}) and suboxic (red, O_2 < 5 µmol L^{-1}) areas in the 1851 to 2100 period in NEMO-PISCES historical and future RCP8.5 simulations.

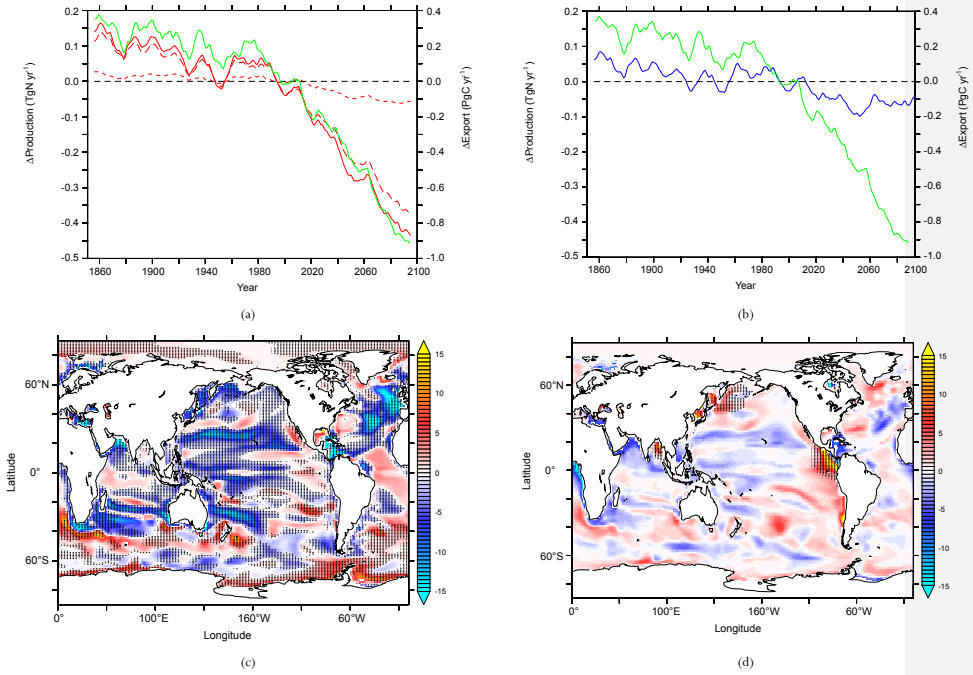

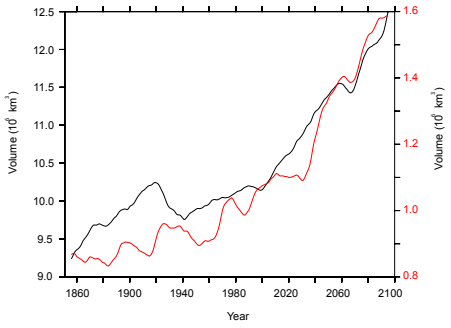
12.5
12.0
11.5
11.0
10.5
10.0
9.5
9.0
Volume (10^6 km^3)
1.6
1.4
1.2
1.0
0.8
Volume (10^6 km^3)
1860
1900
1940
1980
2020
2060
2100
Year

(e)

972
973

974 Fig 6: (a) Anomalies in N_2O inventory (in TgN) from 1851 to 2100 in P.TEMP (blue) and
975 P.OMZ (red) using the historical and future RCP8.5 simulations in the upper 1500m. Change
976 in vertically integrated N_2O concentration (in mgN m^{-2}) in the upper 1500m using NEMO-
977 PISCES model mean from the averaged 2080-2100 to 1985-2005 time periods in future
978 RCP8.5 and historical scenarios respectively in (b) P.TEMP and (c) P.OMZ. Hatched areas
979 indicate regions where the annual mean mixed layer depth is reduced by more than 5m in
980 2080-2100 compared to 1985-2005.

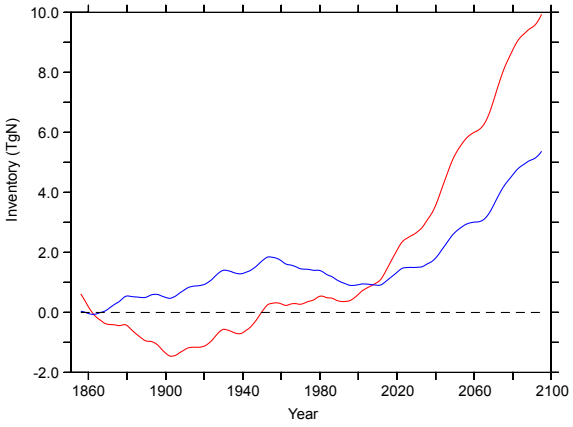

981
982 (a)
983

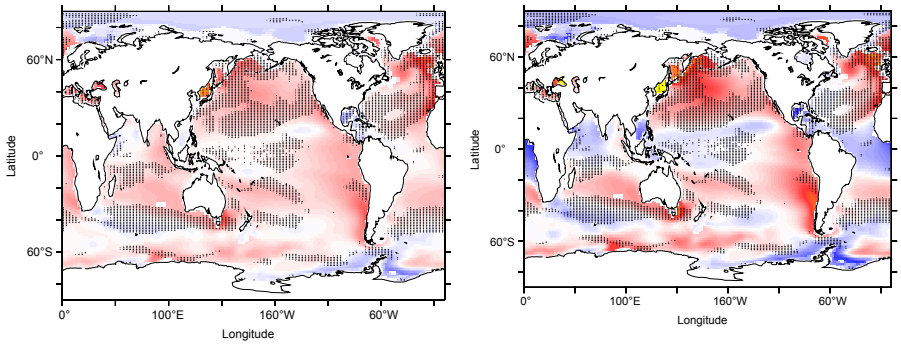

(b) (c)

984
985

Fig. 7: Change in the whole water column in N_2O sea-to-air flux (blue), high-O_2 production pathway (red), low-O_2 production pathway (orange), total N_2O production (yellow) and N_2O inventory (green) for P.OMZ from the averaged 2080-2100 to present 1985-2005 averaged time period in the NEMO-PISCES historical and future RCP8.5 simulations (based on Mikaloff-Fletcher et al. (2006) oceanic regions).

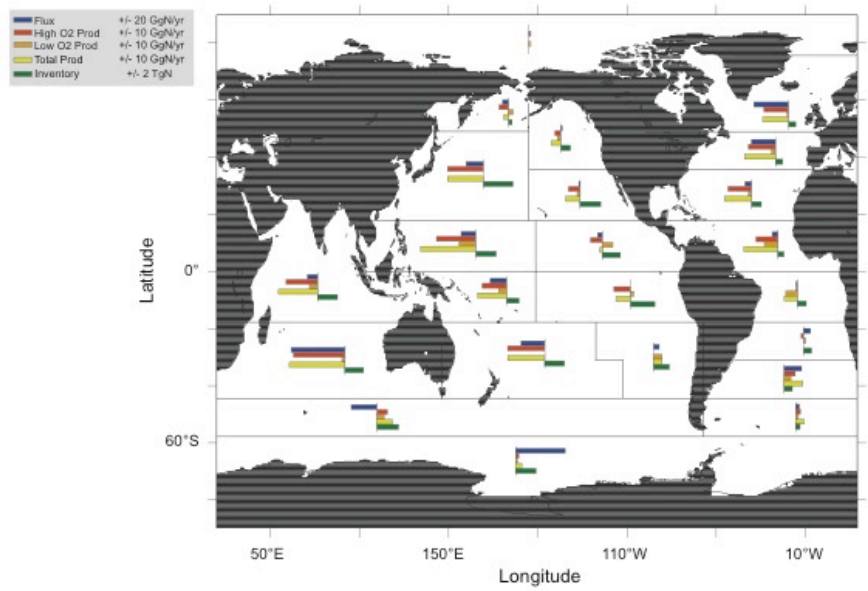

Figure 8: Distribution of O_2 concentration in NEMO-PISCES 1985 to 2005 averaged time period (black) compared to the oxygen-corrected World Ocean Atlas (red) from Bianchi et al. (2012). Interval widths are O_2 concentrations at steps of 5 µmol L^{-1}.

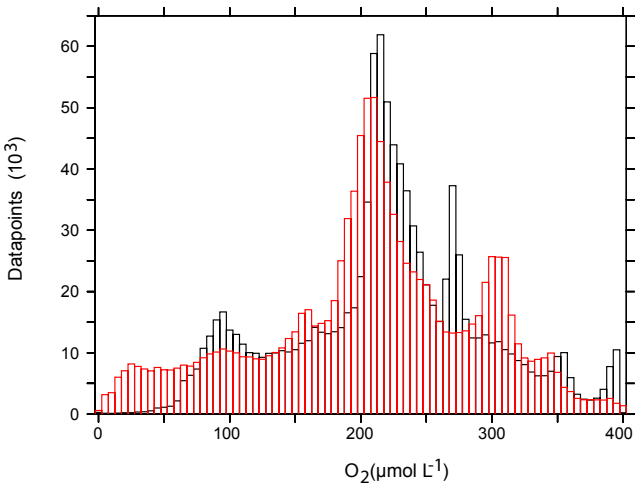

Jorge 5/8/15 8:02 PM
Deleted: Fig. 8: Box model results, analyzing the effect of changes in ocean circulation by reducing the mixing coefficient (µ in %) and changes in biogeochemistry by reducing export of organic matter (in %) separately in N_2O sea-to-air emissions and N_2O inventory in 2100. (**a**) Constant regimes in percentage of the historical N_2O sea-to-air flux: 95% pink, 90% blue, 85% cyan and 80% green, and (**b**) Constant regimes in percentage of the historical N_2O concentration in the deep: 90% pink, 110% blue, 125% cyan and 150% green.

Jorge 5/8/15 8:02 PM
Deleted:

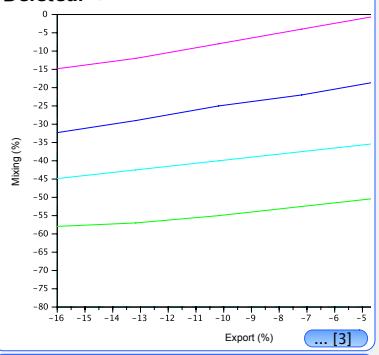

Jorge 5/8/15 8:01 PM
Deleted: 9

Figure 9: Averaged O_2 concentration between 200-600m depth (in µmol L^{-1}) (left) and export of carbon (in mmolC m^{-2} d^{-1}) (right) in (**a**) WOA2005* and Dunne et al. (2007), (**b**) CMIP5 model mean historical simulations over the 1985-2005 time period and (**c**) NEMO-PISCES for the present 1985-2005 time period.

Jorge 5/8/15 8:01 PM
Deleted: 10

a. WOA2005* and Dunne et al., 2007

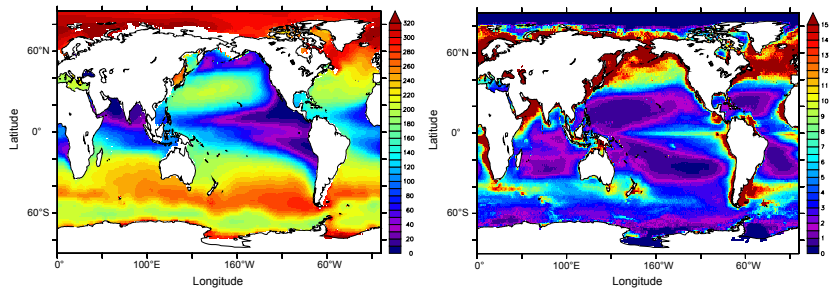

b. CMIP5 model mean

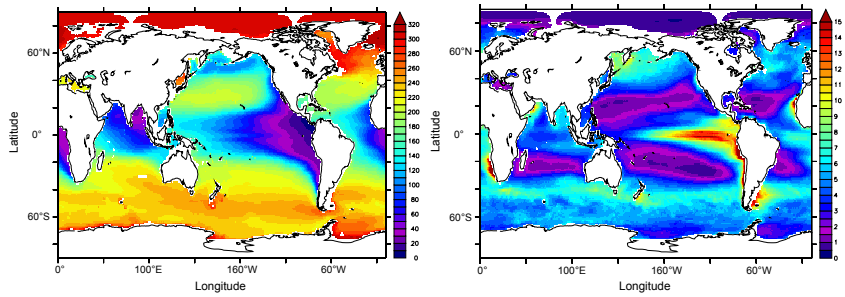

c. NEMO-PISCES

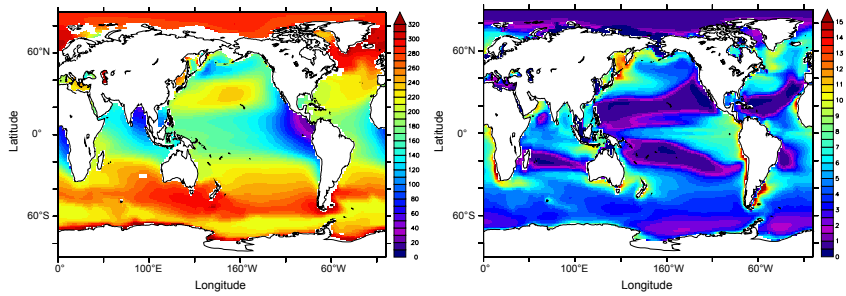

SUPPLEMENTARY MATERIAL

The O_2 modulation fuction $f(O_2)$ in P.OMZ is defined as,

$$f(O_2) = \begin{cases} \dfrac{O_2}{O_2^{*1}} & O_2 < O_2^{*1} \\ 1 & O_2^{*1} < O_2 < O_2^{*2} \\ 0.7 \cdot exp - 0.5(O_2 - O_2^{*2})/O_2^{*2} + \\ 0.3 \cdot exp - 0.05(O_2 - O_2^{*2})/O_2^{*2} & O_2 \geq O_2^{*2} \end{cases}$$

where O_2^{*1} is 1 µmol L^{-1} and O_2^{*2} is 5 µmol L^{-1}. The shape of the function is shown in Fig. S1.

Fig. S1: Oxygen modulating function $f(O_2)$ in the low-O_2 production pathway term included in P.OMZ from Goreau et al. (1980).

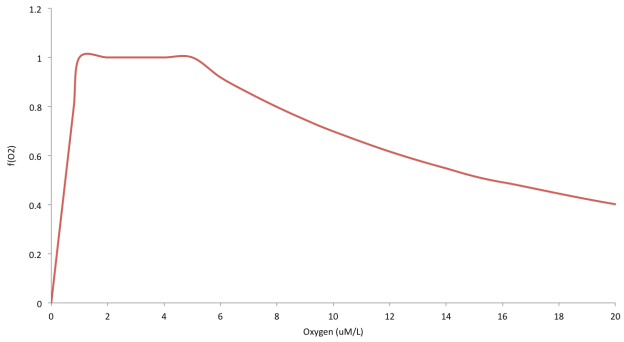

Fig. S2: Vertically integrated (a) high-O_2 and (b) low-O_2 production pathways (in gN m^{-2} yr^{-1}) in P.OMZ for the averaged 1985 to 2005 historical simulation.

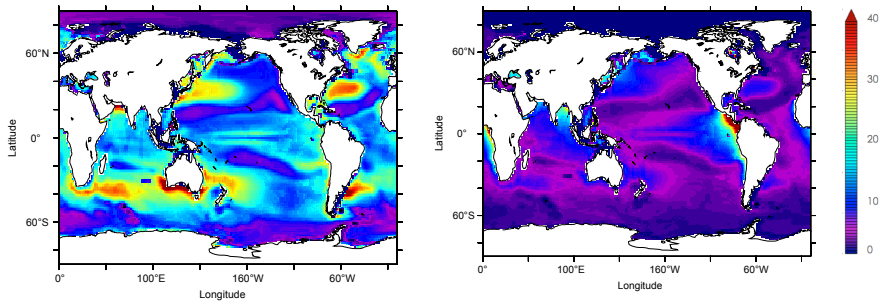

(a) (b)

1042

1043

Jorge 5/8/15 8:01 PM

Deleted: Fig. S3: Diagram of the box model. N_2O inventory is separated into surface and deep concentrations above and below 100m. The fraction of N_2O outgassed to the atmosphere (k), mixing ratio (r) between deep and surface and the rate of N_2O production from the export of organic matter to depth (e) regulate the N_2O budget in the ocean interior. ... [4]